Parameter Free Prediction of Rheological Properties of Homopolymer Melts by Dynamic Monte Carlo Simulation

ARTICLE *in* MACROMOLECULES · NOVEMBER 2012

Impact Factor: 5.8 · DOI: 10.1021/ma301307d

3 AUTHORS:

John R. Dorgan
Colorado School of Mines
94 PUBLICATIONS **2,036** CITATIONS
SEE PROFILE

Nicholas A. Rorrer
Colorado School of Mines
8 PUBLICATIONS **18** CITATIONS
SEE PROFILE

Christopher Maupin
Colorado School of Mines
35 PUBLICATIONS **580** CITATIONS
SEE PROFILE

Macromolecules

Article

pubs.acs.org/Macromolecules

Parameter Free Prediction of Rheological Properties of Homopolymer Melts by Dynamic Monte Carlo Simulation

John R. Dorgan,* Nicholas A. Rorrer, and C. Mark Maupin

Department of Chemical and Biological Engineering, Colorado School of Mines, 1500 Illinois Street, Golden, Colorado 80401, United States

ABSTRACT: A biased Monte Carlo method is developed to simulate shear flow of linear homopolymers between neutral hard walls. Simulations are conducted on a face-centered cubic (FCC) lattice at full occupancy ($\varphi = 1$) using a modified version of Pakula's cooperative motion (COMOTION) algorithm. As chain lengths are increased under quiescent conditions, a clear crossover in chain dynamics from Rouse behavior to reptation-like behavior is revealed in characteristic correlation functions. Shear flow is simulated through the use of a biasing technique that favors segmental movement in the direction of flow; this combination of cooperative motion with flow is referred to as the COMOFLO algorithm. Using this technique, rheological properties are calculated as a function of shear rate and chain length. The viscosity and the first and second normal stress coefficients are calculated and found to be consistent with well-established experimental facts. The zero-shear viscosity scales linearly with low molecular weights ($\eta_0 \sim N^{1.0}$) and scales to the 3.5 power at higher molecular weights ($\eta_0 \sim N^{3.5}$). This crossover in viscosity scaling occurs at the same chain lengths ($N \sim 150$) as the transition in chain dynamics. Because the simulations are conducted in the athermal limit, there are *no* parameter inputs. The known observable linear viscoelastic rheological properties of polymer melts are thus predicted in an *a priori* fashion.

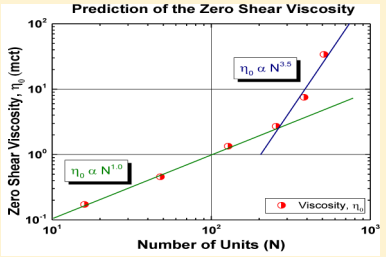

I. INTRODUCTION

Computer simulations are being employed in many areas of research and have gained widespread success across many disciplines of study. In polymer science various simulations have produced results that agree with experiments and have already found practical use. There have been many approaches applied to studying polymers and their properties, each with its own advantages and disadvantages. The use of molecular dynamics is very powerful due to its ability to predict properties based only on interaction potentials.[1] However, MD simulations are very computationally expensive; accordingly, many coarse-graining techniques have been proposed. Coarse-graining techniques include Brownian dynamics and Monte Carlo methods.[2−8]

Brownian dynamics (BD) has been successfully utilized to study various complex polymer systems.[9−20] In BD simulations, polymers are modeled as bead and spring systems subject to random forces as a means of capturing Brownian motion. These studies range from observing the relaxation in various polymer models[17,18] to studying the configuration and rheological dynamics of molecules under shear and other types of flow[9−12,15,16] and even to the study of DNA.[13,14,19,20] BD simulations have proven useful in mapping real chain architectures onto coarse-grained models.

Many studies examine the dynamics of polymer chains using Monte Carlo (MC) techniques. Many of the previous dynamic Monte Carlo (DMC) studies, such as those conducted by Kreitmeier et al.,[21] Nelson et al.,[22] and Schulz et al.,[23] show reptation-like signatures in the response of the center-of-mass motion. In the work done by Paul et al.[24,25] the bond fluctuation algorithm is used to show a crossover in dynamic correlation functions from Rouse to reptation behavior as the length of the polymer chains is increased. Furthermore, in a seminal paper by Shaffer,[26] a variant of the bond fluctuation algorithm was developed where it is possible to turn "on" and "off" chain entanglements. When chains are allowed to cross, the entanglements are turned "off" and untangled Rouse dynamics are shown for all chain lengths. However, when chains are not allowed to cross, and thus the entanglements are turned "on", the chains exhibit reptation-like behavior (in the scaling of the diffusion coefficient with molecular weight) at longer chain lengths.

Some studies also show a direct correspondence between molecular dynamics and Monte Carlo simulations.[6,8,23,27−29] In these studies the authors directly demonstrate that the dynamics of polymer systems are reproduced in both atomistic molecular dynamic studies and corresponding coarse-grained Monte Carlo simulations; diffusion coefficients maintain their proper scaling. Importantly, these studies show better agreement between Monte Carlo and molecular dynamic simulations when a face-centered cubic (FCC) lattice is used.[28] (This improved agreement may be due to the higher coordination number ($Z = 12$) provided by an FCC lattice.) Accordingly, it can be concluded that previous studies demonstrate that dynamic Monte Carlo can be used to capture realistic chain dynamics across the molecular weight span from unentangled to entangled regimes.

Received: June 25, 2012
Revised: October 15, 2012
Published: October 24, 2012

Nonequilibrium molecular dynamics (NEMD) and nonequilibrium (biased) dynamic Monte Carlo (NEMC) techniques have been used to study polymer flows. In a founding paper on biased Monte Carlo, Katz et al. present a rigorous method for biasing the classic Ising model to simulate an external electric field.[30] Deuring and Rabin[31,32] reported early results of biased Monte Carlo simulations of polymers in simple shear and Poiseuille flow in two dimensions between impenetrable walls. Additionally, a previous three-dimensional DMC study[33] replicates the salient features of Poiseuille flow of polymers using a biasing technique similar to the present study. Lai and Binder[34] use a biasing of the probability of the jump rates as a function of box position to simulate the shear flow of polymers. These authors show that a variety of properties, such as the radius of gyration, are affected by shearing. But this technique is not able to accurately reproduce a linear velocity profile; a nonlinear velocity profile exists close to the "no-slip" boundary.

In a series of studies done by Yang et al.,[35−39] the authors model chains under various flow conditions using the bond fluctuation algorithm. In a seminal paper on shear flow[35] the group calculates an effective viscosity which scales to the power of 1.3 relative to the number of beads minus one $(N - 1)$ (i.e., $\eta_{\text{eff}} \sim (N - 1)^{1.3}$). This work generates the correct linear velocity profile for shear flow but is only able to obtain data for low occupancies of the lattice. Limitations of this early work include use of a two-dimensional lattice, lack of a higher density representative of polymer melts, and application only to short chain lengths. In a subsequent publication[36] on shear flow, the Yang group simulates shear flow in three dimensions; a linear velocity profile is again obtained. However, in this work the authors do not report on the rheological properties of the system, and their work only models a dilute solution of polymers.

In a study by Huh and Balazs,[40] the authors show shear thinning behavior for telechelic chains under flow of different functionalities. In a later publication by Li and Denn[41] the authors study extensional flow of dilute polymer solutions and are able to compare the results to those obtained using BD simulations.

In a recent study of shear flow, Jeszka and Pakula[42] use biased dynamic Monte Carlo. These authors define multiple different ways to obtain a shear flow profile including moving both walls of the simulation box in opposite directions, or moving one wall, while the other wall is kept stationary. The authors are able to generate a linear velocity profile at high shear rates, but at lower shear rates they are not able to produce the correct linear flow profile often demonstrating nonlinearities at the walls. Since these authors are not able to simulate the linear flow profile, the shear rate is not constant. This precludes a rigorous calculation of *bona fide* rheological properties. An extended NVT ensemble, in which the shear rate is held constant, is required to enable the rigorous calculation of rheological properties.

In a relevant MD study by Kroger and Hess[1] the relation between chain size and the scaling of zero shear viscosity is presented. Specifically, the correct crossover of zero shear viscosity with increasing molecular weight is obtained. The zero shear viscosity scales with molecular weight to the first power $(\eta_0 \sim N^{1.0})$ at low molecular weights and with a power between 3.0 and 3.5 in the higher molecular weight regime $(\eta_0 \sim N^{3.0}$ to $\eta_0 \sim N^{3.5})$. However, the authors also reported that their simulations are very time intensive, taking *over a year on a 64 processor computer* to complete.

The study presented here offers a number of improvements over previous approaches by using a modified version of Pakula's cooperative motion algorithm.[3−5,43,44] This new methodology, cooperative motion with flow (COMOFLO), produces a linear velocity profile, thereby fulfilling the requirement of an extended ensemble of constant shear rate. Also, a fully occupied lattice more physically representative of polymer melts is possible. Most importantly, the present methodology is extremely computationally efficient; all results presented were obtained on a single processor desktop PC. Rheological properties for linear homopolymers are calculated, and the behavior of these functions is consistent with an enormous amount of data on a large number of experimental systems.[45−48] Because the simulation technique is parameter free, it is concluded that the new methodology enables the *a priori* prediction of the well-known rheological properties for linear homopolymers. As such, the present approach should be capable of being extended to address a wide variety of issues in the rheology of polymer melts, including a greater understanding of the effects of molecular weight distribution and chain architecture on the rheological properties of complex polymer mixtures.

II. METHODOLOGY

A. Simulation Method. MC simulations of linear homopolymers are performed on a face-centered cubic (FCC) lattice by the use of a modified version of Pakula's cooperative motion algorithm.[4,5,43,44] Bond lengths are constant and equal to $(2a)^{1/2}$, where a is the lattice constant. The coordination number of the FCC lattice is 12, and there are four permissible bond angles: 180°, 120°, 90°, and 60°. In this algorithm, which has already been presented extensively in the literature,[3−5,43,44] chain segments move and replace neighboring segments, so that cooperative motion can occur. These movements abide a set of rules in which excluded volume, chain connectivity, and bond length are all preserved.

In the simulations presented in this study periodic boundary conditions are specified in the y and z directions, while a solid "wall" boundary is specified in the x direction, at $x = 0$ and $x = L$. The minimum wall spacing in the simulations is at least 10 times the unperturbed radius of gyration to ensure an adequate system size and reduce confinement effects. A schematic of the simulation is presented in Figure 1. Simulations are performed using chains that have N segments with N ranging from 16 to 512 as described by Table 1.

B. Time Step Implementation. To calculate velocity profiles and the dynamic correlation functions, a fundamental

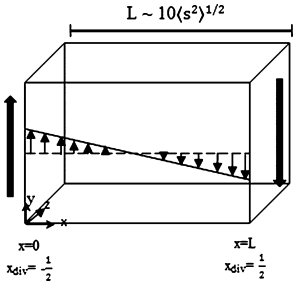

Figure 1. Schematic representation of simulation box showing the coordinate system.

dx.doi.org/10.1021/ma301307d | *Macromolecules* 2012, 45, 8833−8840

Table 1. Case Studies[a]

N	L	y, z	N_{chains}	$\langle R^2\rangle_0^{1/2}$	$\langle S^2\rangle_0^{1/2}$
16	32	16	256	6.1	2.6
48	48	24	288	11.0	4.5
64	48	24	216	12.7	5.2
128	96	48	864	15.5	6.3
256	96	48	432	17.9	7.3
384	128	60	600	25.3	10.3
512	160	80	1000	35.8	14.6

[a]Number of chain segments, N; nonperiodic box lengths, L; periodic dimensions in the y and z directions, total number of chains, and quiescent end-to-end vectors, $\langle R^2\rangle_0^{1/2}$, and radii of gyrations, $\langle S^2\rangle_0^{1/2}$.

time step must be assigned. Time steps are assigned to algorithmic moves that mimic conformation isomerization of polymer chains. Following Mansfield and Theodorou,[49] the fundamental time step, tu, is defined as

$$tu = \frac{1}{N_{segments}} \tag{1}$$

where $N_{segments}$ is the total number of segments on the lattice (the number of chains times the segments per chain, N). If n_{moves} is the number of Monte Carlo moves, then when $tu \cdot n_{moves} = 1$ on average each segment in the box has experienced an attempted displacement.

Time is incremented once for each local movement completed. These local moves include an end bond rotation, a crankshaft-like motion around two bonds, kink straightening/formation, and displacement of a few segments along the chain contour. Full details of these elementary moves is outlined in the sixth chapter of *Simulation Methods for Polymers*.[44]

C. Flow Biasing. In order to simulate shear flow, the Monte Carlo moves are biased. As previously stated, the FCC lattice has 12 nearest neighbors. On the FCC lattice, four of the nearest neighbors represent a step in the forward ($+y$ direction), four represent a step backward ($-y$ direction), and the remaining four represent a lateral step in the y-plane. In the case of quiescent diffusion, where no flow biasing is present, there is an equal probability that a move can occur in the forward, backward, or lateral y direction corresponding to a probability of 4/12 or 1/3 for each direction.

To simulate shear flow, the random walk of segmental displacements must be biased. To accomplish this biasing, the system is defined as shown in Figure 1 so that flow velocity is zero at the midplane and greatest in magnitude near the walls. This is done by defining a position in the box, x_{div}, as

$$x_{div} = \frac{x}{nx + 1} - \frac{1}{2} \tag{2}$$

where nx is the distance between the hard walls in the x-direction and x is the location in the box, both measured in lattice units. This new coordinate thus defines x_{div} as $-1/2$ at the left wall, 1/2 at the right, and 0 at the middle when viewed as depicted in Figure 1.

The probabilities of taking a step in the forward, p_{+y}, and backward direction, p_{-y}, respectively are

$$p_{+y} = p_{zero}(1 - p_{max}x_{div}) \tag{3}$$

$$p_{-y} = p_{zero}(1 + p_{max}x_{div}) \tag{4}$$

where p_{zero} is the probability of making a move in any y direction with no biasing present (i.e., $p_{zero} = 1/3$) and p_{max} is the biasing parameter that sets the strength of the shearing. That is, p_{max} determines the magnitude of the shear rate. The sum of the probabilities for motion in the y direction is unity as they include $p_y = p_{zero}$ corresponding to lateral motion. If p_{max} is zero, then $p_{+y} = p_{-y} = p_y = p_{zero} = 1/3$ is recovered for all Monte Carlo steps, and no flow occurs. When a nonzero value for p_{max} is set, the probability of displacing a segment in the negative y direction is greatest at the right wall and equal in magnitude to the probability of displacing a segment in the positive y direction at the left wall leading to the velocity profile depicted in Figure 1 (see Figure 4 also).

Sampling of the system is conducted in a method similar to Owicki and Scheraga[50] and Gleiman and Dorgan,[33] where trial moves are made by the following steps:

(a) Generate a random number, *rand*, uniformly between 0 and 1.
(b) Compare the random number to the numerical divisions set by p_y, p_{+y}, and p_{-y}.
(c) Make a trial move in the direction prescribed by the biasing parameter determined in (b) (i.e., if $0 \le \text{rand} \le p_{-y}$, then attempt backward moves with equal random probability; if $p_{-y} < rand \le p_y + p_{-y}$, then attempt lateral moves with equal random probability; if $p_y + p_{+y} < rand \le p_y + p_{-y} + p_{+y}$ (=1), then attempt forward moves with equal random probability).
(d) If the trail move is acceptable, make the move, increment time, and update the configuration. Otherwise, increment time, generate a new random number, and repeat the process.

In every simulation the velocity profile, radius of gyration, end-to-end vector, order parameters, chain end distribution, correlation functions, and the components of the stress tensor are periodically recalculated by averaging over several hundreds of thousands of closed loop cooperative motion displacements.

One type of starting configuration consists of the chains laid out in all-trans configurations on the lattice. Monte Carlo moves are performed with no flow biasing present in order to "melt" or equilibrate this initial configuration. To track this equilibration, the radius of gyration is monitored as a function of Monte Carlo time until it reaches a steady state average value. When an all-trans configuration is used, a typical equilibration would consist of 1.5 million closed loop moves. Depending on the box size in Table 1, this can take as little as 1 h and no more than 48 h on a single Intel i5 processor. Once the biasing is applied, the same procedure is used to track the equilibration under flow biasing. Monte Carlo moves are performed until a linear velocity profile is obtained, and the box-averaged radius of gyration reaches a constant value. Such steady-state configurations may also be used for the initial configuration based on p_{max} values that are either smaller or greater than the case of interest. Results were checked to ensure that the type of initial configuration utilized did not affect the results obtained. Some improvement (decrease) in the Monte Carlo time needed for reaching steady state is observed when utilizing initial configurations from steady-state configurations having similar p_{max} values.

D. Calculation of Rheological Properties. The shear rate, $\dot{\gamma}$, is defined as the derivative of velocity in the y direction with respect to the x direction or

dx.doi.org/10.1021/ma301307d | Macromolecules 2012, 45, 8833−8840

$$\dot{\gamma} = \frac{dv_y}{dx} \tag{5}$$

where v_y is the velocity in the y direction and the x is the position in the box. As shown below, the velocity profile obtained is linear meaning that the shear rate is constant.

The stress tensor is calculated from the dyadic product of the bond vectors. In this system, the total stress tensor, $\underline{\underline{\sigma}}$, is calculated from[47]

$$\underline{\underline{\sigma}} = 2\nu kT\beta^2\langle \underline{r}\underline{r}\rangle \tag{6}$$

where k is the Boltzmann constant, T is temperature, and $\langle \underline{r}\underline{r}\rangle$ is the dyadic product of the bond vectors. Furthermore, by using Kramer's bead−spring treatment, ν is defined as the number of chains per unit volume and β^2 is defined as $3/(2Nl^2)$, where l is the length of a Kuhn segment. Thus, dimensionless stress is

$$\frac{\underline{\underline{\sigma}}}{2\nu kT} = \frac{3\langle \underline{r}\underline{r}\rangle}{2Nl^2} = \frac{3\langle \underline{r}\underline{r}\rangle}{2\langle R^2\rangle} \tag{7}$$

where $\langle R^2\rangle$ is the unperturbed, unconfined end-to-end vector. This value has previously been determined[51] for the present lattice model with no bond energies as

$$\langle R^2\rangle^{1/2} = 1.58N^{0.5} \tag{8}$$

Individual components of stress follow as

$$\frac{\sigma_{xy}}{2\nu kT} = \frac{3\langle r_x r_y\rangle}{2\langle R^2\rangle} \tag{9}$$

for the shear stress, σ_{xy}, and

$$\frac{\sigma_{xx}}{2\nu kT} = \frac{3\langle r_x r_x\rangle}{2\langle R^2\rangle} \tag{10}$$

for the normal stress, σ_{xx}, in the x direction.

Before the stress is used in rheological calculations, the static stress tensor (where no flow biasing is present) corresponding to the thermodynamic pressure is subtracted from the total stress tensor to give the deviatoric stress tensor, $\underline{\underline{\tau}}$.

Finally, with the shear rate and dimensionless stress data, the viscosity, the first and second normal stress differences, and the first and second normal stress coefficients can be calculated according to eqs 11−15.

$$\eta = \frac{\tau_{xy}}{\dot{\gamma}} \tag{11}$$

$$N_1 = \tau_{yy} - \tau_{xx} \tag{12}$$

$$N_2 = \tau_{xx} - \tau_{zz} \tag{13}$$

$$\Psi_1 = \frac{N_1}{\dot{\gamma}^2} \tag{14}$$

$$\Psi_2 = \frac{N_2}{\dot{\gamma}^2} \tag{15}$$

Here η is the viscosity, N_1 and N_2 are the first and second normal stress differences, and Ψ_1 and Ψ_2 are the first and second normal stress coefficients, respectively.

III. RESULTS AND DISCUSSION

A. System Dynamics (Rouse and Reptation). One of the hallmarks of the cooperative motion algorithm is that it simulates polymer chains at high densities (full lattice occupancy) in three dimensions. At these realistic densities proper implementation of the time stepping enables the simulation technique to capture Rouse and reptation-like dynamics for short and long chains, respectively. Chain dynamics are described by a series of correlation functions. These functions, where $r_i(t)$ is the position of a given bead in the box at time t and $r_{cm}(t)$ is the center of mass of the polymer chain, include the mean-squared displacement of central monomers

$$g_1(t) = \langle [r_i(t) - r_i(t=0)]^2\rangle \quad \text{for } i = \frac{N}{2} \tag{16}$$

the mean-squared displacement of central monomers in center of mass coordinates

$$g_2(t) = \langle [(r_i(t) - r_{cm}(t)) - (r_i(t=0) - r_{cm}(t=0))]^2\rangle \quad \text{for } i = N/2 \tag{17}$$

the mean-squared center of mass displacement

$$g_3(t) = \langle [r_{cm}(t) - r_{cm}(t=0)]^2\rangle \tag{18}$$

the mean-squared displacement of chain ends

$$g_4(t) = \langle [r_i(t) - r_i(t=0)]^2\rangle \quad \text{for } i = 1 \text{ and } i = N \tag{19}$$

and the mean-squared displacement of chain ends in center of mass coordinates.

$$g_5(t) = \langle [(r_i(t) - r_{cm}(t)) - (r_i(t=0) - r_{cm}(t=0))]^2\rangle \quad \text{for } i = 1 \text{ and } i = N \tag{20}$$

For lower molecular weights ($N < 150$), Rouse-type behavior is exhibited over three regions of time by observing the g_1 correlation function or the mean-square displacement of chain ends (g_4). At short times these functions scale as $g_1 \sim t$, at intermediate times as $g_1 \sim t^{1/2}$, and finally as $g_1 \sim t$ at longer times scales; results are shown in Figure 2.

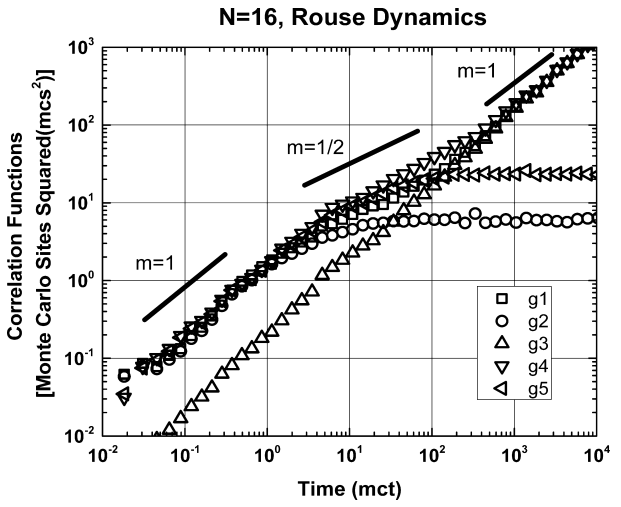

Figure 2. Correlation functions demonstrating Rouse dynamics for an ensemble of $N = 16$ chains.

dx.doi.org/10.1021/ma301307d | Macromolecules 2012, 45, 8833−8840

As the number of segments in the polymer chains increases, the polymers enter a reptation-like regime ($N > 150$). In this regime the mean-squared displacement (g_1) correlation function and the mean-squared displacement of chain ends scales as $g_1 \sim t^{1/2}$ at low time scales, as $g_1 \sim t^{1/4}$ at intermediate times, and as $g_1 \sim t^{1/2}$ at longer times. Characteristic results are presented in Figure 3. The inset graph shows strong evidence of the reptation like dynamic behavior in g_1; lines of the appropriate slopes have been drawn through the data.

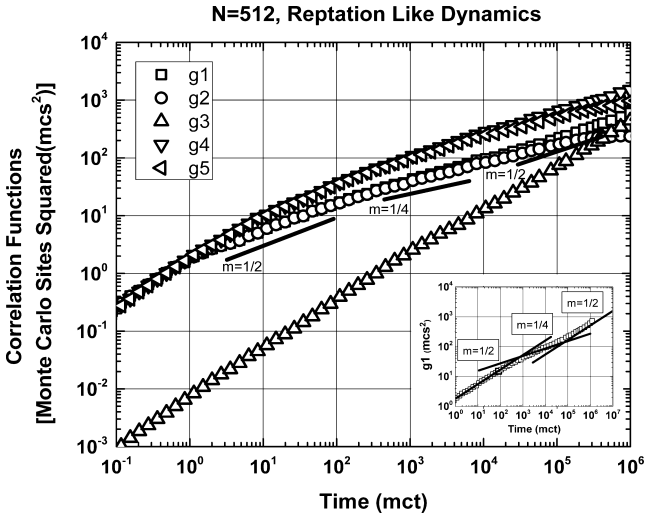

Figure 3. Correlation functions demonstrating reptation-like dynamics for an ensemble of $N = 512$ chains; inset clearly shows.

In the context of the reptation model the changes in scaling are associated with particular time and length scales. The transition from $g_1 \sim t^{1/2}$ to $g_1 \sim t^{1/4}$ occurs at the entanglement time, τ_e. At this time, the central monomers have diffused the diameter of the tube so their mean-squared displacements should be on the order of the tube diameter (a) squared, $g_1 \approx a^2$ (more exactly,[52] the crossover occurs when $g_1 = {}^1/_3 a^2$ and $t^* = (\pi^3/36)\tau_e$).

The data show continuous transitions rather than abrupt shifts so times can only be estimated by reading the points from the straight lines of the inset of Figure 3. The data show this first transition at a time around $t^* \approx 1000$ mct steps ($t^* = 844$ mct) corresponding to $\tau_e = 981$ mct. At this time, $g_1 = 51.9$ mcs^2. In the reptation picture this implies a tube diameter of $a = 12.5$ mcs. Similarly, the transition from $g_1 \sim t^{1/4}$ to $g_1 \sim t^{1/2}$ occurs at the Rouse time, τ_R. This time is estimated to be about $\tau_R = 7 \times 10^4$ mct. At this time, g_1 is given by $g_1 = abN^{1/2}$, where b is the Kuhn step length of eq 8. Good consistency is evidenced with the reptation picture assuming the value of $g_1 = 200$ mcs^2 at $\tau_R = 7 \times 10^4$ and $a = 12.5$ mcs; this calculation provides a value of $b = 0.71$, which is in rough agreement with eq 8.

This dynamic crossover and reptation-like dynamics occur because the cooperative motion algorithm captures physically realistic chain movements. In dense liquid media, cooperative motion is known to occur, and local cooperative movements constitute the basis of Pakula's COMOTION algorithm. In the literature, many models and algorithms capture the Rouse dynamics of a system. However, since these other models have limits on the amount of occupied lattice sites in order to give reasonable acceptance rates, they are difficult to use to model reptation-like dynamics, especially for longer chain lengths such as the $N = 512$ case presented here.

B. Velocity Profile. Velocity is calculated by tracking the displacement of segments at each lattice position as a function of Monte Carlo time. Segmental displacements are recorded, and the sum of the displacements is divided by the current Monte Carlo time to provide a calculated velocity. At short times, or a low number of attempted Monte Carlo moves, the simulation is not yet fully equilibrated to the linear velocity profile. In about a trillion attempted moves (only a couple of hours on a single processor) the simulation reaches a steady velocity profile which does not change as the number of biased moves is increased. An example velocity profile equilibration is shown in Figure 4.

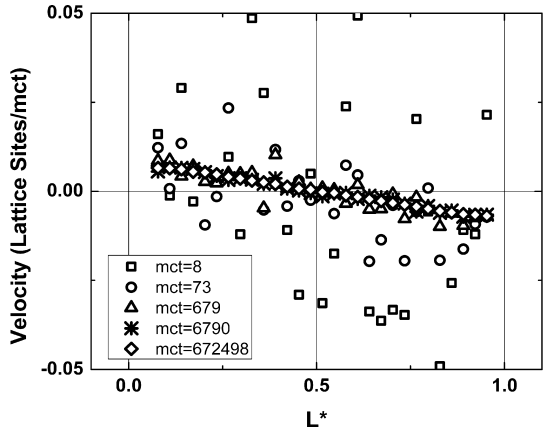

Figure 4. Emergence of the constant velocity profile as a function of Monte Carlo time (mct) for the $N = 64$ case and an applied bias of $p_{max} = 7 \times 10^{-2}$.

The biased simulation methodology results in a linear velocity profile. As demonstrated in Figure 5, the gradient of the velocity profile (the shear rate) can be adjusted by changing the biasing parameter. Previous attempts made with the cooperative motion algorithm[42] showed difficulties in obtaining the requisite linear velocity profiles. This error seems most pronounced when the velocity is defined to be zero at one wall and a maximum at another wall.[34,42] The key feature of the present approach is that it does provide the requisite linear

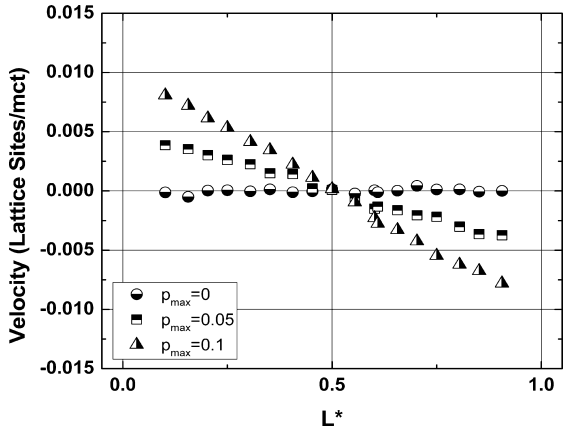

Figure 5. Velocity profiles as a function of the biasing parameter, p, for an $N = 256$, $L = 128$ system. Here L^* is defined as x/L.

dx.doi.org/10.1021/ma301307d | Macromolecules 2012, 45, 8833−8840

velocity profile which is shown for two nonzero values of the biasing parameter in Figure 5. The shear rate for a given simulation is found by fitting the respective velocity profile to a straight line.

Figure 6 shows that for a constant chain length the shear rate is a linear function of the biasing parameter p_{max}, as might be

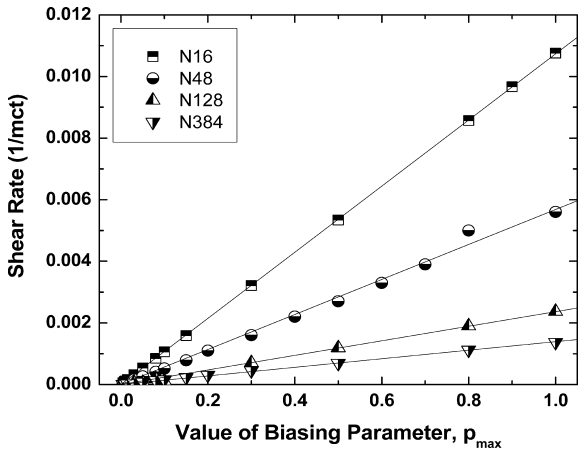

Figure 6. Shear rate as a function of the user set biasing parameter and coarse-grained chain units.

expected; the shear rate is also a function of chain length. As the number of coarse-grained segments increases, the shear rate decreases (Figure 6). In this respect, the biasing parameter p_{max} acts like a shear stress; the higher the molecular weight of the polymer chain, the greater the biasing parameter (stress) needed to obtain a given shear rate.

C. Rheological Response. Figure 7 show a typical response of the biasing technique. At low shear rates the

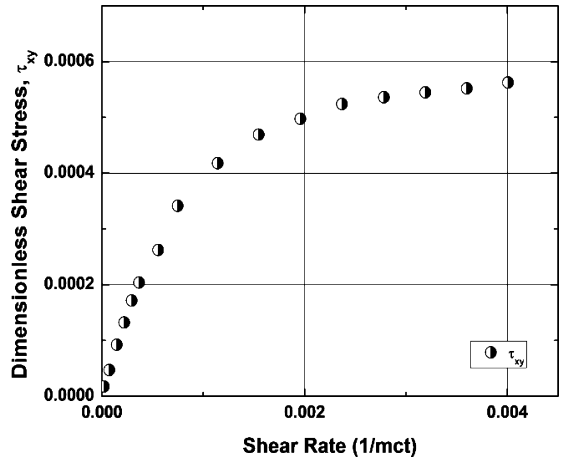

Figure 7. Shear stress as a function of shear rate for the $N = 48$ case.

chains do not align in the direction of flow; they can relax on the time scale of the deformation, and a constant viscosity is observed. At higher shear rates chain relaxation is slower than the time scale for deformation, and chains become aligned; the proportionality between the calculated shear stress and the shear stress changes. That is, at low shear rates the viscosity is a constant, but at higher shear rates the viscosity decreases. This is the classic shear-thinning behavior associated with the flow of polymer melts.

The calculated viscoelastic functions show the universal behavior typical of polymeric liquids. Using appropriate values of the stress tensor, it is possible to calculate the rheological properties defined by eqs 11−15. Figure 8 presents the first and

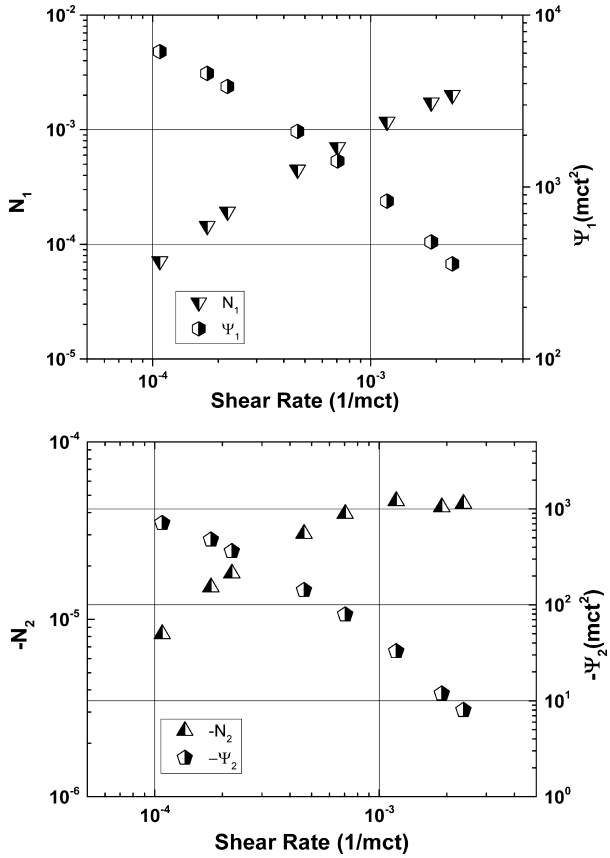

Figure 8. First and second normal stress differences (left axis) and their coefficients (right axis) as a function of shear rate for the $N = 128$ case.

second normal stress differences (N_1 and N_2) and the first and second normal stress coefficients (Ψ_1 and Ψ_2—shown on the right-hand axes) as a function of shear rate for $N = 128$. As with real polymer melts, the first normal stress difference is opposite in sign to the second normal stress difference. Also, the second coefficient is smaller in magnitude than the first. With increasing shear rate both the first and second normal stress differences increase, while the first and second normal stress coefficients decrease. Importantly, Figure 9 shows that as the shear rate is decreased the ratio of the second to the first stress difference approaches the asymptotic value of about 0.1. This value has been observed in a wide number of literature reports on polymer rheology.[47] *In fact, all of the simulation results are consistent with known experimental facts for linear homopolymers.*

The results of the simulations show classic pseudoplastic behavior. At low shear rates the viscosity is constant until a critical shear rate is reached after which the polymer begins to shear thin. Viscosity as a function of shear rate for three different chain lengths is presented in Figure 10. Note that all three curves collapse at high shear rates onto the asymptote with a slope of roughly −2/3; this means the power-law index for the model chains is in the vicinity of 1/3, which is again consistent with the values found for a large number of synthetic polymers.

dx.doi.org/10.1021/ma301307d | *Macromolecules* 2012, 45, 8833−8840

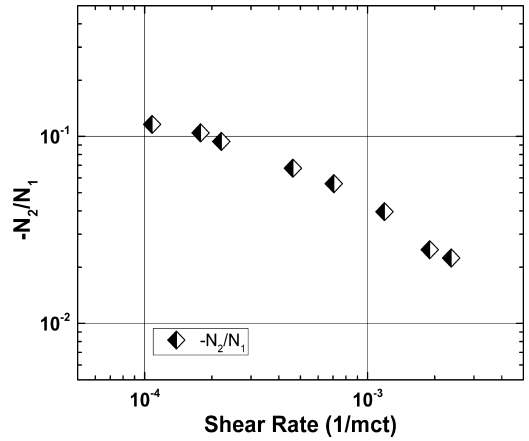

Figure 9. Ratio of the second to first normal stress differences as a function of shear rate for the $N = 128$ case.

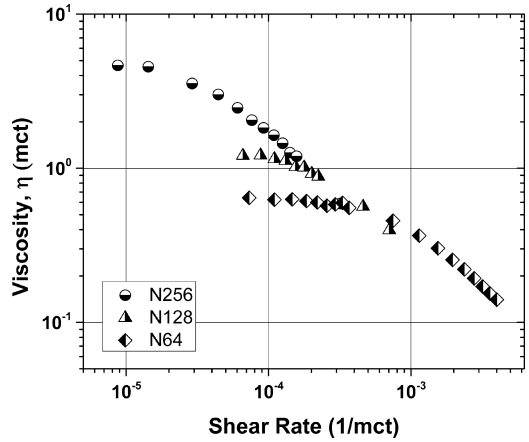

Figure 10. Shear viscosity as a function of shear rate for various molecular weights.

For all calculations the zero-shear viscosity is calculated by averaging the viscosity values before the critical shear rate. With increasing molecular weight (chain length N), the onset of shear thinning occurs at lower characteristic shear rates; the inverse of this shear rate can be considered a characteristic relaxation time which increases with increasing N as expected. In addition, the viscosity collapses onto a single curve at very high rates corresponding to segmental dynamics.

In addition to capturing accurate melt flow dynamics, the simulation also captures two distinct regions in the scaling of zero-shear viscosity with molecular weight. This result is shown in Figure 11. The new COMOFLO simulation technique obtains the correct scaling for the zero shear viscosity, η_0, as a function of molecular weight. In the Rouse regime ($N < 150$) the zero shear viscosity is proportional to the molecular weight to the first power ($\eta_0 \sim N^{1.0}$). Where reptation-like behavior is seen ($N > 150$) the zero-shear viscosity scales as molecular weight to the 3.5 power ($\eta_0 \sim N^{3.5}$). Two distinct regimes of zero-shear viscosity have been observed experimentally for a variety of polymers.[48] Kroger and Hess[1] also observe this same scaling for their NEMD simulations; they report the zero shear viscosity scaling to the 1 power ($\eta_0 \sim N^{1.0}$) at lower molecular weights and that the zero-shear viscosity scales with a power between 3.0 and 3.5 ($\eta_0 \sim N^{3.0}$ to $\eta_0 \sim N^{3.5}$) at higher molecular weights. However, as mentioned previously, their

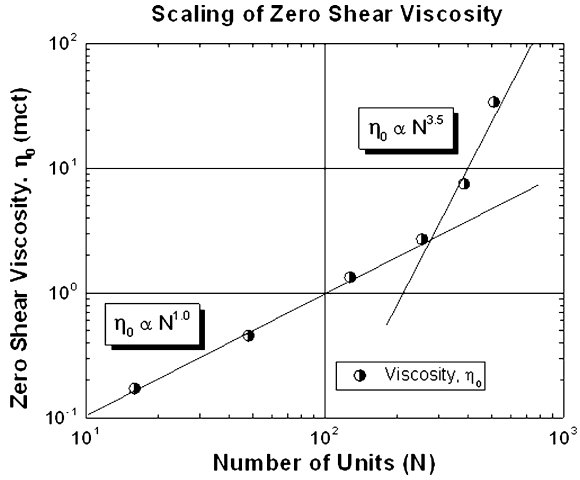

Figure 11. Scaling of zero shear viscosity as a function of the number of chain segments, N.

approach is *tens of thousands* of times more computationally expensive than the present technique.

IV. CONCLUSIONS

A powerful new nonequilibrium dynamic Monte Carlo methodology has been developed which enables the *a priori* prediction of the rheological properties of homopolymer melts. This approach combines cooperative motion with probabilistic segmental biasing to create flow and is called the COMOFLO algorithm. Preliminary calculations on linear chains are fully consistent with the known experimental facts. The technique thus holds great promise for predicting the flow properties of differing chain architectures and their mixtures. Present investigations are focused on the effects of molecular weight distribution and topological variations in chain architectures on melt rheology.

Shear flow is simulated using a modified version of the cooperative motion algorithm. These Monte Carlo simulations are performed on a face-centered cubic (FCC) lattice at full occupancy. This simulation method accurately captures the dynamics of polymer melts under quiescent conditions. The Rouse and reptation regime are evident at low and high molecular weights, respectively. These regimes are observed in the mean-squared displacement of central monomers (g_1) or the mean-squared displacement of chain ends (g_4) correlation functions. Rouse-like dynamics are observed for chains shorter than 150 ($N < 150$) in which the g_1 and g_4 correlation functions scale as t^1 at short times, $t^{1/2}$ at intermediate times, and t^1 at longer times. Reptation-like dynamics are observed for chains longer than 128 ($N > 150$), in which g_1 and g_4 scale as $t^{1/2}$ at short times, $t^{1/4}$ at intermediate times, and $t^{1/2}$ at longer times.

In order to simulate shear flow, the random walk of segments is biased. Hard walls are defined in the x direction, while periodic boundary conditions are maintained in the y and z directions. The distance between the hard walls is defined to be at least 10 times the unperturbed radius of gyration. In the middle of the box there is an equal probability of a segment moving in any direction and the probability of moving backward is greatest at the right wall and equal in magnitude to the probability of stepping forward at the left wall. The biasing methodology results in a linear velocity profile and thus a constant shear rate. Because of the constant shear rate extended ensemble, other quantities such as the viscosity, the

dx.doi.org/10.1021/ma301307d | Macromolecules 2012, 45, 8833−8840

first and second normal stress coefficients, and the first and second normal stress difference can be calculated. All of the calculated quantities, as well as the scaling of zero-shear viscosity with molecular weight, are found to be consistent with well-known experimental facts. Because the model involves no free parameters, the universal melt flow behavior of polymer melts has been predicted in a fully *a priori* manner.

AUTHOR INFORMATION

Corresponding Author

*E-mail: jdorgan@mines.edu.

Notes

The authors declare no competing financial interest.

ACKNOWLEDGMENTS

This work was funded by the Fluid Dynamics Program of the National Science Foundation under grant CBET-1067707. The authors thank the reviewers for a number of valuable suggestions.

DEDICATION

This paper is dedicated to the memory of Professor Tadeusz Pakula.

ABBREVIATIONS

DMC, dynamic Monte Carlo; CMA, cooperative motion (COMOTION) algorithm; COMOFLO, cooperative motion with flow; mct, Monte Carlo time; mcs, Monte Carlo sites; NEMD, nonequilibrium molecular dynamics; FCC, face-cntered cbic; MD, molecular dynamics.

REFERENCES

(1) Kroger, M.; Hess, S. *Phys. Rev. Lett.* **2000**, *85*, 1128−1131.
(2) Binder, K.; Paul, W. *J. Polym. Sci., Part B: Polym. Phys.* **1997**, *35*, 1−31.
(3) Gauger, A.; Weyersberg, A.; Pakula, T. *Makromol. Chem., Theory Simul.* **1993**, *2*, 531−560.
(4) Geyler, S.; Pakula, T.; Reiter, J. *J. Chem. Phys.* **1990**, *92*, 2676−2680.
(5) Pakula, T. *Macromolecules* **1987**, *20*, 679−682.
(6) Deutsch, H. P.; Binder, K. *J. Chem. Phys.* **1991**, *94*, 2294−2304.
(7) Tries, V.; Paul, W.; Baschnagel, J.; Binder, K. *J. Chem. Phys.* **1997**, *106*, 738−748.
(8) Haire, K. R.; Carver, T. J.; Windle, A. H. *Comput. Theor. Polym. Sci.* **2001**, *11*, 17−28.
(9) Andrews, N. C.; McHugh, A. J.; Schieber, J. D. *Macromol. Theory Simul.* **1998**, *7*, 19−26.
(10) Andrews, N. C.; McHugh, A. J.; Schieber, J. D. *J. Rheol.* **1998**, *42*, 281−305.
(11) Doyle, P. S.; Shaqfeh, E. S. G.; Gast, A. P. *J. Fluid Mech.* **1997**, *334*, 251−291.
(12) Doyle, P. S.; Shaqfeh, E. S. G.; McKinley, G. H.; Spiegelberg, S. H. *J. Non-Newtonian Fluid Mech.* **1998**, *76*, 79−110.
(13) Hur, J. S.; Shaqfeh, E. S. G.; Larson, R. G. *J. Rheol.* **2000**, *44*, 713−742.
(14) Larson, R. G.; Hu, H.; Smith, D. E.; Chu, S. *J. Rheol.* **1999**, *43*, 267−304.
(15) Li, L.; Larson, R. G.; Sridhar, T. *J. Rheol.* **2000**, *44*, 291−322.
(16) Larson, R. G. *J. Non-Newtonian Fluid Mech.* **2000**, *94*, 37−45.
(17) Ghosh, I.; McKinley, G. H.; Brown, R. A.; Armstrong, R. C. *J. Rheol.* **2001**, *45*, 721−758.
(18) Grassia, P.; Hinch, E. J. *J. Fluid Mech.* **1996**, *308*, 255−288.
(19) Jendrejack, R. M.; de Pablo, J. J.; Graham, M. D. *ICCN 2002: Int. Conf. Comput. Nanosci. Nanotechnol.* **2002**, 111−114.
(20) Jendrejack, R. M.; de Pablo, J. J.; Graham, M. D. *J. Chem. Phys.* **2002**, *116*, 7752−7759.
(21) Kreitmeier, S.; Wittkop, M.; Trautenberg, H. L.; Holzl, T.; Goritz, D. *J. Comput. Phys.* **1997**, *133*, 181−185.
(22) Nelson, P. H.; Hatton, T. A.; Rutledge, G. C. *J. Chem. Phys.* **1997**, *107*, 1269−1278.
(23) Schulz, M.; Winkler, R. G.; Reineker, P. *Phys. Rev. B* **1993**, *48*, 581−584.
(24) Paul, W.; Binder, K.; Heermann, D. W.; Kremer, K. *J. Phys. II* **1991**, *1*, 37−60.
(25) Paul, W.; Binder, K.; Heermann, D. W.; Kremer, K. *J. Chem. Phys.* **1991**, *95*, 7726−7740.
(26) Shaffer, J. S. *J. Chem. Phys.* **1994**, *101*, 4205−4213.
(27) Carmesin, I.; Kremer, K. *Macromolecules* **1988**, *21*, 2819−2823.
(28) Downey, J. P.; Crabb, C. C.; Kovac, J. *Macromolecules* **1986**, *19*, 2202−2206.
(29) Baschnagel, J.; Binder, K.; Doruker, P.; Gusev, A. A.; Hahn, O.; Kremer, K.; Mattice, W. L.; Muller-Plathe, F.; Murat, M.; Paul, W.; Santos, S.; Suter, U. W.; Tries, V. *Adv. Polym. Sci.* **2000**, *152*, 41−156.
(30) Katz, S.; Lebowitz, J. L.; Spohn, H. *J. Stat. Phys.* **1984**, *34*, 497−537.
(31) Duering, E.; Rabin, Y. *Macromolecules* **1990**, *23*, 2232−2237.
(32) Duering, E.; Rabin, Y. *J. Rheol.* **1991**, *35*, 213−219.
(33) Gleiman, S. S.; Dorgan, J. R. *J. Chem. Phys.* **2000**, *112*, 6073−6083.
(34) Lai, P. Y.; Binder, K. *J. Chem. Phys.* **1993**, *98*, 2366−2375.
(35) Xu, G. Q.; Ding, J. D.; Yang, Y. L. *J. Chem. Phys.* **1997**, *107*, 4070−4084.
(36) Xu, G. Q.; Ding, J. D.; Yang, Y. L. *Polymer* **2000**, *41*, 3289−3295.
(37) Xu, G. Q.; Ding, J. D.; Yang, Y. L. *Macromol. Theory Simul.* **1998**, *7*, 129−140.
(38) Xu, G. Q.; Ding, J. D.; Yang, Y. L. *Rheol. Acta* **1999**, *38*, 562−568.
(39) Xu, G. Q.; Ding, J. D.; Yang, Y. L. *Rheol. Acta* **2001**, *40*, 60−66.
(40) Huh, J.; Balazs, A. C. *J. Chem. Phys.* **2000**, *113*, 2025−2031.
(41) Li, X. F.; Denn, M. M. *J. Rheol.* **2004**, *48*, 805−821.
(42) Jeszka, J. K.; Pakula, T. *Polymer* **2006**, *47*, 7289−7301.
(43) Pakula, T. *J. Chem. Phys.* **1991**, *95*, 4685−4690.
(44) Kotelyanskii, M.; Theodorou, D. N. In *Simulation Methods for Polymers*; Marcel Dekker: New York, 2004; pp 147−176.
(45) Graessley, W. W. *Polymeric Liquids and Networks: Structure and Properties*; Garland Science: Oxford, 2003.
(46) Graessley, W. W. *Polymeric Liquids and Networks: Dynamics and Rheology*; Garland Science: Oxford, 2008.
(47) Larson, R. G. *Constitutive Equations for Polymer Melts and Solutions*; Butterworths: New York, 1988.
(48) Ferry, J. D. *Viscoelastic Properties of Polymers*; Wiley: New York, 1980.
(49) Mansfield, K. F.; Theodorou, D. N. *Macromolecules* **1989**, *22*, 3143−3152.
(50) Owicki, J. C.; Scheraga, H. A. *Chem. Phys. Lett.* **1977**, *47*, 600−602.
(51) PaiPanandiker, R. S.; Dorgan, J. R.; Pakula, T. *Macromolecules* **1997**, *30*, 6348−6352.
(52) Likhtman, A. E.; McLeish, T. C. B. *Macromolecules* **2002**, *35*, 6332−6343.